FT-IR analysis of pure C3S hydration in diluted solutions and effect of graphene oxide on the hydrated products

Paolo Gronchi[1,a], Marco Goisis[2,b], Stefania Bianchi[1,c]

[1]*Chemistry, Materials, and engineering Chemistry (CMIC), Politecnico di Milano, Milano, Italy*
[2]*Global Product Innovation Dept., HeidelbergCement, i.lab, Bergamo, Italy*

[a]paolo.gronchi@polimi.it
[b]m.goisis@itcgr.net
[c]stefania.bianchi29@gmail.com

ABSTRACT

Tricalcium silicate, i.e. C3S, is the most abundant constituent of Portland cement and it accounts for the early strength development of hydrated cement. Studying the kinetics and mechanism of its hydration can lead to a better understanding of the morphology of the final product, i.e. C-S-H, and thus to a higher chance of influencing the resulting cement properties.

Graphene oxide is an oxidized form of graphene, laced with oxygen-containing groups. Its hydrophilic behaviour permits to disperse it into hydraulic matrices to modify morphology and performance of the hydrated products. At first, the research delves into the hydration of C3S over time, with the purpose of following the development of C-S-H morphologies and identifying some chemical and physical parameters that can affect them; then, it focuses on the effect of graphene oxide on C3S dissolution and relevant C-S-H product. The investigation is based mainly on FT-IR spectroscopy highlighting the peaks emerging at increasing reaction times. Complementary used instrumental techniques are SEM, Raman and thermal analyses (TGA and DSC). The spectroscopic analysis is particularly addressed at the infrared range between 900 and 1100 cm-1, that is characteristic of the absorption of polymerized SiO2 and C-S-H as well. By confining the investigation to the simple C3S/H2O system we intend to get mainly qualitative results on the interaction of C-S-H, both kinetics and morphology, with GO and explore the possibility to modify the nanostructure of cement.

1. INTRODUCTION

Graphene is the "wonderful material" of these years and it is not surprising that the Flagship of research in Europe is there waving. Many academic and industrial fields, from electronics to batteries and super-capacitors, from clothing to composite, from 3D printing to flexible displays are investigating the opportunities offered by this material. In this framework, researchers on materials for the construction industry, one of the largest industry worldwide, with a production of 4.1 billion tons in 2016 (as reported by Cembureau), are exploring graphene as an opportunity for improving the mechanical performances of cementitious materials. First of all, carbon nanomaterials are considered of high value to improve performance and durability of the cement matrix, because of their high strength (Lee et al. (2008) reported a Young's modulus of 1.0 TPa and an intrinsic strength of 130 GPa for a GO monolayer), and then because of their high specific surface area and their effect on porosity, which permits to refine the nano/ microstructure and to have a more homogeneous pore distribution (Li et al. (2015); Yang et al. (2017)). However, not all the results are in complete agreement. For example, according to Chuah et al. (2014) and Lv et al. (2014), graphene oxide (GO) enhances the resistance of cement, since the sheets can bridge microcracks within the matrix and increase strength and toughness, with some reshape of the microstructure and potential positive effect on durability. Horszczaruk et al. (2015) too found that embedment of GO in cement results in significant enhancement of the Young's modulus, but they observed no modifications in the morphology of the products and no effect on the kinetics of hydration. Further differences in behaviour have been reported by Ghazizadeh et al. (2018), who found that GO temporarily retards the hydration of Portland clinker, while it accelerates that of OPC (Ordinary Portland Cement). They attribute this difference to a two-fold behaviour of GO: retardation is due to the interaction of GO with the surface of hydrating clinker grains, which temporarily hinders the formation of precipitation nuclei, while this doesn't occur with OPC, because of the seeding effect of gypsum on sulphate ions. It is important to observe that GO has oxygen-containing polar functionalities (epoxy, carboxyl, hydroxyl) that may enhance the interaction with the hydrated products and improve the dispersion. Use of polycarboxylate superplasticizer and ultra-sonication process is suggested to help the stabilization of GO dispersion over time (Babak et al. (2014)).In this paper, we investigate the effects of GO addition (0.05%, 0.10%, 0.20% and 0.30% by weight of solid) on C-S-H formation, starting from the single phase C_3S, which is the most abundant component of Portland clinker. C-S-H is the core product of hydrated cement and is responsible for most of the mechanical and durability properties of the final material. In this study, we adopt a very simple model, with a high water-to-solid ratio, according to fundamental studies on the subject (Haas and Nonat (2014); He et al. (2014)). Previous preliminary studies performed in Politecnico di Milano, CMIC laboratory (Romani (2015)), have permitted to optimize the instrumental investigation on cement–GO composites by Raman and SEM analysis. This work integrates with two previous research works on a system based on (C+S) and on C_2S respectively, of which the present study uses the same experimental conditions.

2. EXPERIMENTAL PROCEDURE

2.1 Materials

Alite was supplied by Italcementi HeidelbergCementGroup. C_3S is the main component of OPC and it hydrates according to (1):

$$C_3S + H_2O \rightarrow C\text{-}S\text{-}H + CH \tag{1}$$

where C-S-H is the typical notation used in the cement world for the calcium silicate hydrated products and CH for portlandite ($Ca(OH)_2$). C_3S size was: D10= 3.39 μm, D50=11.8 μm and D90=127 μm, with a Blaine specific surface area of 3190 cm^2/g.

Graphene oxide (GO), 4 mg/ml aqueous dispersion, was provided by Graphenea Inc., San Sebastian, Spain. Its monolayer content was higher than 95% and its oxygen content was 41-50%. A dispersing PCE comb-polymer, based on an acrylic backbone 30% grafted with chains of PEG 1000) was added to the aqueous system to increase GO dispersion. Reagent grade potassium thiocyanate (KSCN) was used for infrared analysis.

2.2 Compositions

Five different combinations of C_3S with water and GO were prepared: the compositions are reported in Table 1. High diluted dispersions, water to cement ratio equal to 50 (wt/wt), were adopted (Haas and Nonat (2014)). PCE concentration in water was more than one order of magnitude lower than corresponding typical concentration in basic cementitious mixtures (paste/mortar) and therefore assumed negligible on hydration kinetics.

Table 1. The compositions of C_3S samples

Sample code	C_3S (g)	Water (g)	Dispersant (wt. % in water)	Graphene Oxide (wt. % in C_3S)
C_3S-Control	2.000	100	0.009	0
C_3S-GO-0.05	2.000	100	0.009	0.05
C_3S-GO-0.10	2.000	100	0.009	0.10
C_3S-GO-0.20	2.000	100	0.009	0.20
C_3S-GO-0.30	2.000	100	0.009	0.30

The samples were prepared by mixing the demineralized water, the GO and the dispersant in a glass beaker. To improve the GO dispersion, the beaker was placed inside an ultrasonic bath at 59 KHz for 30 min at 285 W. C_3S was added to the liquid mixture, which was kept for 4 weeks under continuous mechanical agitation in a jacketed reactor at controlled temperature (25°C).

Samples were collected from the reactor at 2 hours, 24 hours, 48 hours, 1 week, 2 weeks, 3 weeks and 4 weeks, and occasionally at further time intervals. The samples were centrifuged at 4000 rpm for 5 min and the supernatant removed. After that, a solution of methanol and acetone (50/50) was added to the cement paste, to halt the hydration reaction. Eventually, to dry the samples, they were placed inside a water-pump mild-vacuum oven, operating at room temperature for 8 hours.

2.3 Analytical investigations

2.3.1 Infrared and Raman analyses

FTIR spectra were recorded using a Nexus Nicolet FT-IR spectrometer (Nicolet Instrument. Inc., Madison, WI 53711, USA) coupled with an infrared microscope Continuμm Thermo Electron Corporation (GMI, Inc, Ramsey, Minnesota, USA). Spectra were acquired in transmission mode using KBr pellet pressed under vacuum (300 mg of KBr, 1 mg of dried product and 0.25 mg (precisely weighed) of KSCN as reference for quantitative evaluation).

Raman analyses were performed by Horiba Jobin Yvon Labram HR800 (HORIBA Jobin Yvon IBH Ltd., Glasgow, UK) dispersive Raman spectrometer equipped with Olympus BX41 microscope and a 50X objective (resolution, 2 cm^{-1}; acquisition time, 30 s; 4 accumulations). The 785 nm excitation laser line with a power of 0.4 mW was selected in order to prevent possible photo-induced thermal degradation of the samples.

2.3.2 TGA

The instrument was a Seiko Exstar 6000 TG/DTA 6300 thermal analyser (Seiko Instruments Inc., Chiba, Japan). The analyses were carried out in air, from room temperature to 800°C, with constant heating rate of 10°C/min.

2.3.3 SEM

SEM analysis were performed by Zeiss Evo 50 EP instrumentation (Carl Zeiss AG, Oberkochen, Germany) equipped with lanthanum hexaboride (LaB_6) thermoionic source, at 20 kV.

3. EXPERIMENTAL RESULTS AND DISCUSSION

3.1 FTIR spectroscopy

3.1.1 Preliminary analysis

As the intensity of a peak is directly proportional to the amount of the corresponding phase, to get indication of the progress of the reaction, we calculated the ratio between the intensity of the relevant peaks of C-S-H and C_3S. Two peaks were consequently selected to carry out the progress of the reaction: the peak at 963-970 cm^{-1}, attributed to some C-S-H form, and the one at 881 cm^{-1}, attributed to un-hydrated C_3S. With the latter, some inaccuracies might have occurred, as the peak is very close to the carbonates absorption (see Figure 1). Alternative peaks for un-hydrated silica are too weak and noisy to be used for relative measurements. The results, expressed in terms of absorbance ratio, i.e. the ratio between the absorbance at 963-970 cm^{-1} and that at 881 cm^{-1}, within the same spectrum, indicate that the C-S-H/ C_3S ratio tends to raise by increasing the amount of GO, especially at the limit of 0.30% (see Figure 2).
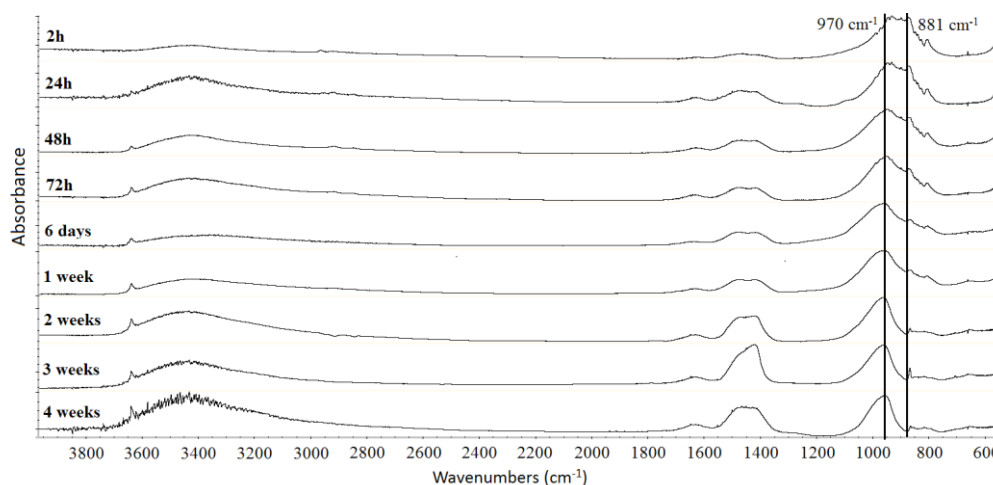

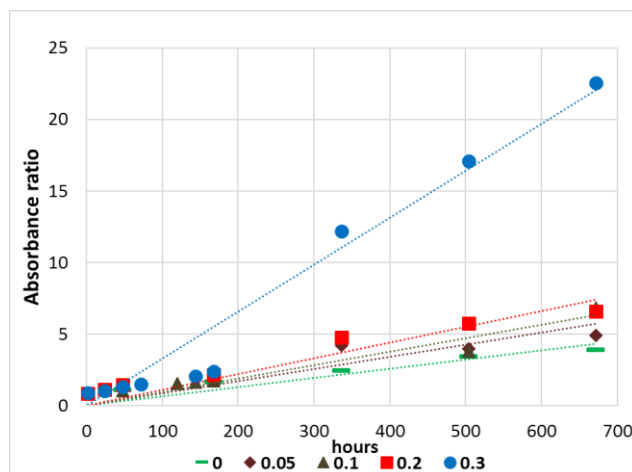**Figure 1. FT-IR spectra at different times, C3S-GO-0.30 sample (0.30% GO)**

Figure 2. Absorbance ratio vs time at different percentages of GO (0, 0.05, 0.1, 0.2 and 0.3) for the reaction of C3S_GO_XX samples.

In order to try and improve the reliability of the kinetic evaluation, the most intense FTIR absorption peak of pure KSCN (the internal standard salt) that did not interfere with those of reagents and products during hydration, was selected, 2068 cm^{-1}.
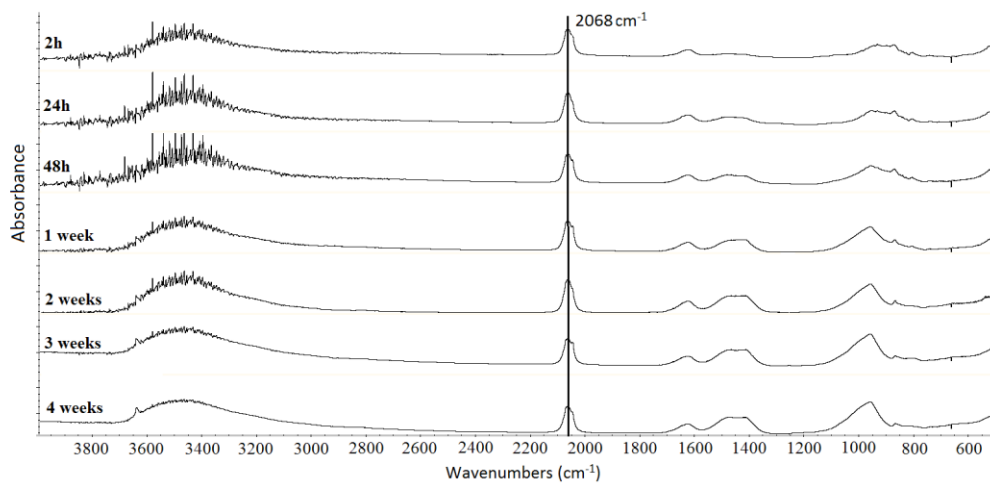
Figure 3. FT-IR spectra at different times, C3S-GO-0.20 samples (0.20% GO) prepared with the standard test salt KSCN

3.1.2 Kinetic investigation

The absorbance of the peak of C-S-H at 963-970 cm⁻¹ was compared to that of the standard by adding the same amount of salt in all the preparations (Figure 4).
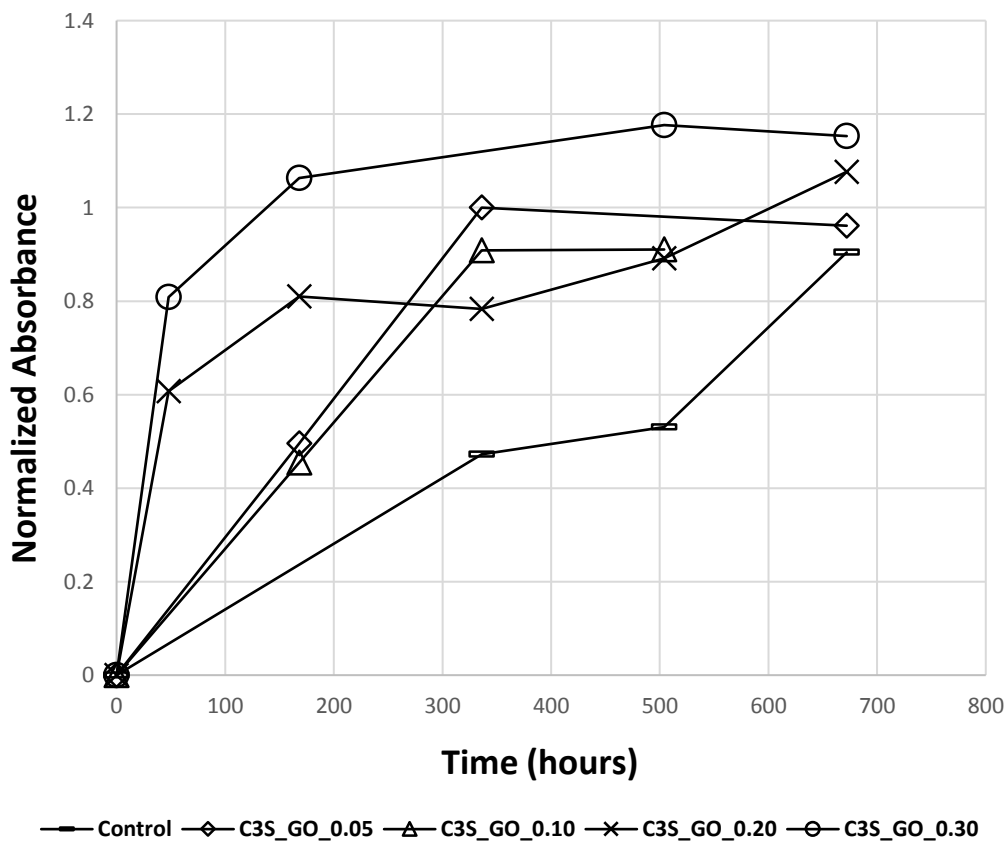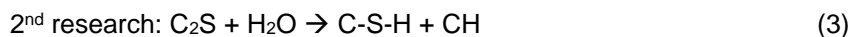

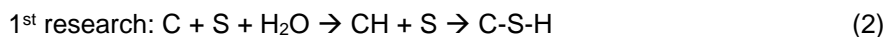**Figure 4. FTIR normalized absorbance at 963-970 cm-1, sample C3S_GO_0.XX**

It is evident from the graph that the samples with GO have higher normalized absorbance than the control, meaning a higher amount of C-S-H at equal hydration time.

Moreover, Figure 4 shows that the rate of hydration of C_3S from the beginning to 7 days as well as the normalized absorbance at 963-970 cm^{-1} at 7 days, depend on the content of GO: the higher the amount of GO (e.g. C3S_GO_0.30), the steeper the tendency curve and the higher the amount of C-S-H. The result is in line with those obtained by other authors regarding the acceleration effect of GO on cement's hydration (Lu et al. (2017)).

3.1.3 Interaction GO-Ca

Graphene oxide interacts to some extent and through different forms, with the dissolved calcium ions in the aqueous dispersion. In fact, in the experiments, GO alone shows very good dispersion in water, but when a little amount of calcium oxide is added, GO rapidly produces flocculation caused by complexation of GO with calcium ions. In order to improve the dispersion, a very low amount of PCE was added to the aqueous composition. In any case, interactions between GO and Ca^{++} remained highly probable with potential reduction of the availability of calcium for the reaction of hydration. This interaction might explain the slowing down of the reaction that resulted in the first research (Gronchi et al. (2018)) and in the second as well (Distefano et al. (2018)) where the reagents to produce C-S-H were (C+S) and C_2S respectively, see (2) and (3):

$$1^{st} \text{ research: } C + S + H_2O \rightarrow CH + S \rightarrow C\text{-}S\text{-}H \qquad (2)$$

$$2^{nd} \text{ research: } C_2S + H_2O \rightarrow C\text{-}S\text{-}H + CH \qquad (3)$$

A possible hypothesis of the different effects of (C+S), C_2S and C_3S on the kinetic of hydration is that C_3S does not interfere negatively with the synthesis of C-S-H because of the greater amount of the available calcium. On the other hand, it may promote the nucleation of C-S-H gel by reactive groups [Han et al. (2017)] with global positive influence on hydration.
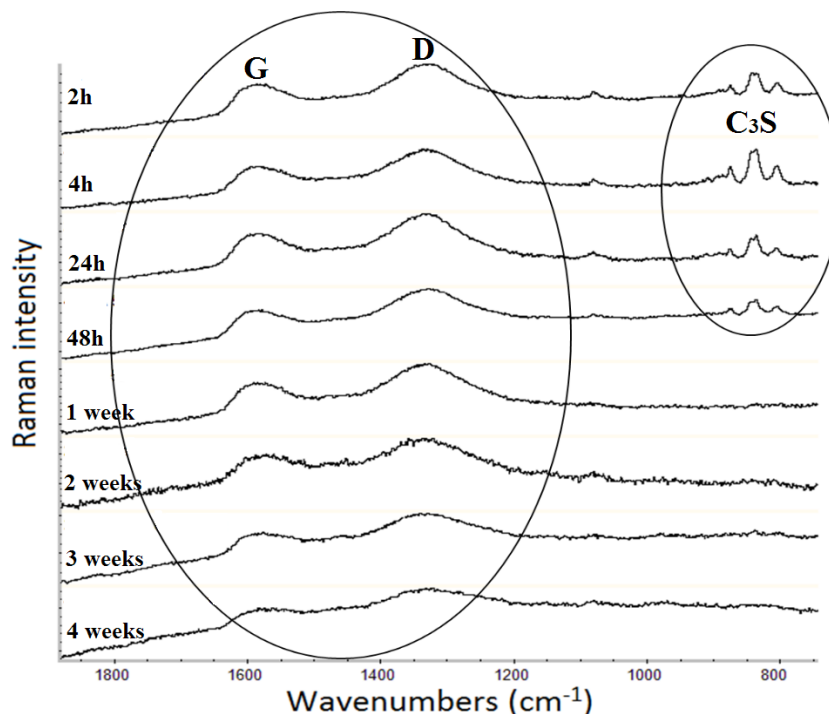
3.2 Raman spectroscopy

Figure 5. **Raman spectra at different times of hydration, C_3S-GO-0.10 sample**.

The wavenumber of the D peak, associated with the out-of-plane vibrations of sp^2 carbons, only occurring with structural defects, is 1350 cm^{-1}, that of the G peak, associated with the in-plane vibrations of sp^2 carbons, is 1580 cm^{-1}. The shape and the intensity ratio between the two peaks are typical of GO.

Their progressive disappearance over time means that GO does not remain separated in the matrix but interacts with it (Ferrari (2007)). The three peaks at 800-880 cm^{-1} are due to the un-hydrated C_3S phases (Ibáñez et al. (2007)), in fact they are only present in the initial stages.

3.3 TGA

Figure 6 and Figure 7 show data collected from the thermogravimetric analyses. The series coded as "Pores water" refers to the range of temperature 150-390°C, while the series "Portlandite" refers to the range 390-500°C. The percentage of water lost in the range 150-390°C is attributed to the water trapped in the pores of C-S-H and to the crystallization water (Taylor (1998)), and hence it can be related to the amount of C-S-H present in the sample. The percentage of water lost in the range 390-500°C is due to the degradation of portlandite, (4):
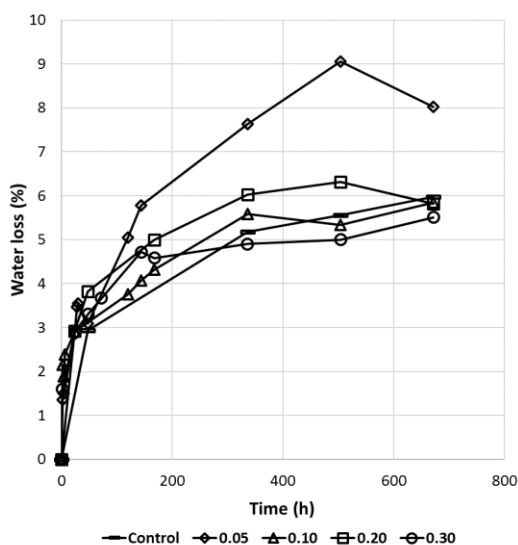
$$Ca(OH)_2 \rightarrow CaO + H_2O \qquad (4)$$

Figure 6. Water loss from pores in the range 150-390°C, (recalculation with zero loss at 150°C)
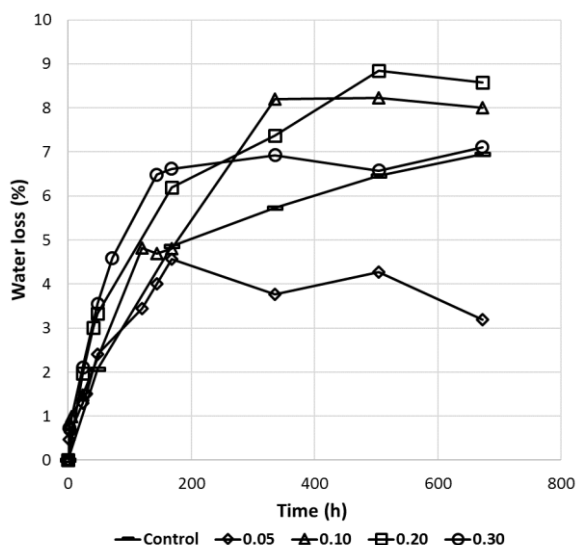
Figure 7. Water loss from portlandite in the range 390-500°C, (recalculation with zero loss at 390°C).

The loss of water from pores and from portlandite as well, are both increasing over time, as expected. Moreover, the slope of the graphs is steeper at the beginning and then it decreases, again as expected. From the data reported in Figure 7, it results that the samples with GO produced more portlandite than the "Control", as suggested by the position of the relative curves, above the reference. Just the C_3S-GO-0.05 curve of the series "portlandite" after one week is surprisingly below the others. It is still unclear whether this is caused by a critical percentage of GO inside C_3S and further investigation is necessary. Moreover, careful examination of the initial trend of the reaction, shows that the effect of the addition of GO is predominant at earlier times of hydration (Lu et al. (2017)).
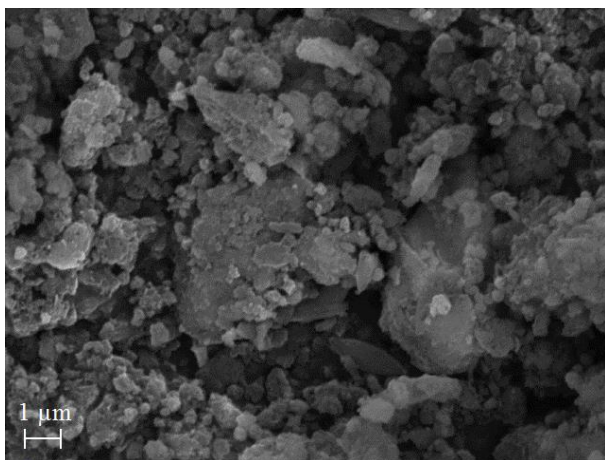
3.4   SEM
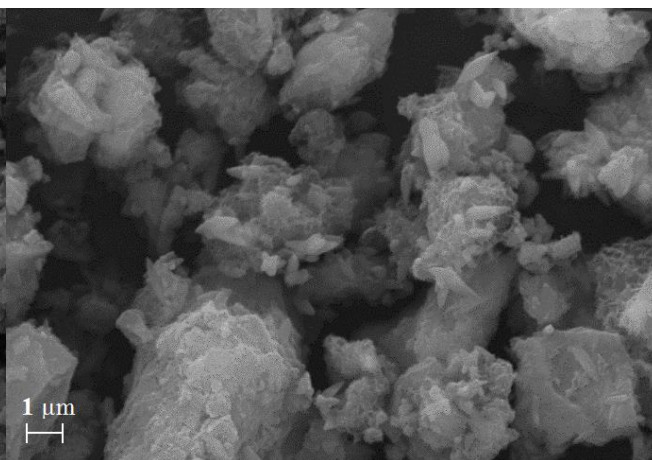

Figure 8. SEM image, Control sample (20k x)
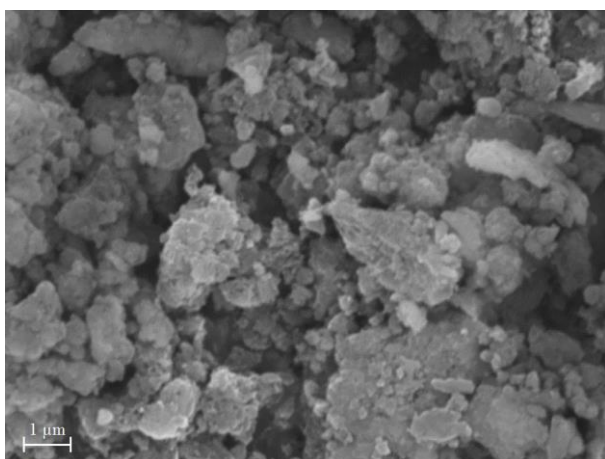

Figure 9. SEM image, C$_3$S-GO-0.05 sample (20k x)

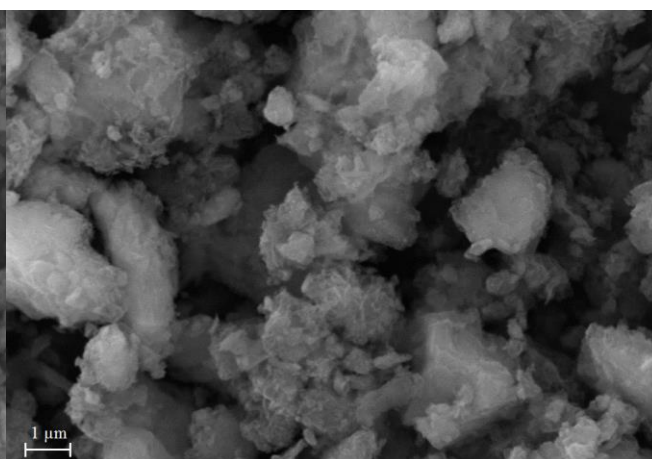**Figure 10. SEM image, Control sample (25k x)**

Figure 11. SEM image, C$_3$S-GO-0.30 sample (25k x)

Figure 8-Figure 11 show SEM photographs taken on samples at 4 weeks of hydration. In
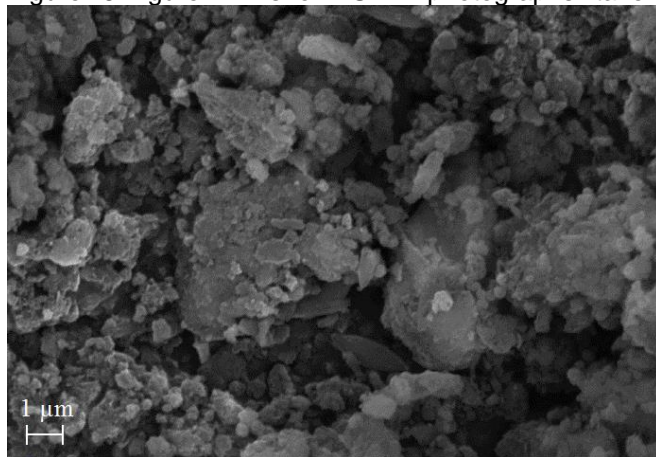
Figure 8, just an amorphous structure with incoherent and shapeless particles is present, probably due to low reactivity and low amount of C-S-H produced. Instead, in Figure 9, the "honeycomb" structure of C-S-H is clearly visible (see also Figure 11), and the structure is more aggregated, indicating a higher amount of C-S-H. The difference from a less hydrated (left, 0% GO) to a more hydrated (right, 0.30% GO) structure is appreciable also in Figure 10 and Figure 11, at a higher magnification. Without GO the material is less aggregated, whereas with 0.30% of GO, it is more compact and some "honeycomb" structures associated to calcium silicates are present. This kind of morphology precedes the formation of elongated fibres and lamellae that intertwine to cooperate to the resistant structure of cement. In the current study, we used a high water/ cement ratio, so the hydrating structures tend to stay separated from each other and this is probably the reason for the formation of the C-S-H "honeycomb" predominant structure.

4. CONCLUSIONS

In previous research carried out starting from (C+S) (Gronchi et al. (2018); Bianchi (2017)) and C_2S (Distefano et al. (2018)), the GO showed a retarding effect on hydration. Instead, the same experimental procedure applied to C_3S and here presented, seems to support the opposite trend. In this case, the presence of GO in the aqueous system (water to solid ratio equal 50:1) led to a slight increase in the kinetics of hydration, as demonstrated by infrared and thermal analyses. An exception is represented by the anomalous result of the sample C3S-GO-0.05 in the range 390-500°C, which might be due to the existence of a hypothetical critical concentration of GO for the system but which needs further investigation to be confirmed. A possible explanation for the different behaviour of the reactions starting from (C+S) and C_2S with respect to that from C_3S might be attributed to the different amount of calcium ions available for the synthesis of C-S-H: it could be argued that because GO links calcium ions, it hinders the hydration reaction when the amount of calcium is limited, i.e. in the case of (C+S) and C_2S. The existence of the interaction between GO and calcium is well supported by literature (Zhao et al. (2016)) and anyway it is plausible because of the polar oxygen functionalities that GO bears. Moreover, the Raman spectra showed that the GO did not remain isolated in the cement matrix, but it interacted with the system itself. The slight acceleration of the hydration with C_3S is probably caused by some prevailing nucleation effect on cement hydrates as already proposed by other authors (Lu et al. (2017)).

5. REFERENCES

Babak F, Abolfazl H, Alimorad R, Parviz G. (2014). *Preparation and mechanical properties of graphene oxide: Cement nanocomposites*. The Scientific World Journal 2014. doi:10.1155/2014/276323.

Bianchi S. (2017). *Study on graphite and graphene oxide as additives in cement: influence on C-S-H formation.* (Thesis) Politecnico di Milano. pp:151.

Chuah S, Pan Z, Sanjayan JG, Wang CM, Duan WH. (2014). *Nano reinforced cement and concrete composites and new perspective from graphene oxide*. Construction and Building Materials 73: 113-124. doi:https://doi.org/10.1016/j.conbuildmat.2014.09.040.

Distefano B, Lemoine B, Sala E, Pillon M, Morandini M, Curti PP. (2018). *Influence of graphene oxide on C2S hydration kinetics*. (Thesis) Politecnico di Milano. pp:38.

Ferrari AC. (2007). *Raman spectroscopy of graphene and graphite: Disorder, electron–phonon coupling, doping and nonadiabatic effects*. Solid State Communications 143(1-2): 47-57. doi:10.1016/J.SSC.2007.03.052.

Ghazizadeh S, Duffour P, Skipper NT, Bai Y. (2018). *Understanding the behaviour of graphene oxide in Portland cement paste*. Cement and Concrete Research 111: 169-182. doi:10.1016/J.CEMCONRES.2018.05.016.

Gronchi P, Bianchi S, Brambilla L, Goisis M. (2018). *Graphite Nanoplatelets and Graphene Oxide Influence on C-S-H Formation*. Published as part of proceedings of the 12th CANMET/ACI International

Conference on Superplasticizers and Other Chemical Admixtures in Concrete in Beijing, China, 28-31 October 2018. ISBN-13: 978-1-64195-029-9 329:237-256. 329:237-256.

Haas J, Nonat A. (2014). *From C–S–H to C–A–S–H: Experimental study and thermodynamic modelling*. Cement and Concrete Research 68:124-138. doi:10.1016/j.cemconres.2014.10.020.

Han B, Zheng Q, Sun S, Dong S, Zhang L, Yu X, Ou J. (2017). *Enhancing mechanisms of multi-layer graphenes to cementitious composites*. Composites Part A: Applied Science and Manufacturing. 101:143-150. doi:10.1016/J.COMPOSITESA.2017.06.016.

He Y, Lu L, Struble LJ, Rapp JL, Mondal P, Hu S. (2014). *Effect of calcium-silicon ratio on microstructure and nanostructure of calcium silicate hydrate synthesized by reaction of fumed silica and calcium oxide at room temperature*. Materials and Structures/Materiaux et Constructions. 47(1-2): 311-322. doi:10.1617/s11527-013-0062-0.

Horszczaruk E, Mijowska E, Kalenczuk RJ, Aleksandrzak M, Mijowska S. (2015). *Nanocomposite of cement/graphene oxide – Impact on hydration kinetics and Young's modulus*. Construction and Building Materials. 78: 234-242. doi:10.1016/J.CONBUILDMAT.2014.12.009.

Ibáñez J, Artús L, Cuscó R, López Á, Menéndez E, Andrade MC. (2007). *Hydration and carbonation of monoclinic C2S and C3S studied by Raman spectroscopy*. Journal of Raman Spectroscopy. 38(1): 61-67. doi:10.1002/jrs.1599.

Lee C, Wei X, Kysar JW, Hone J. (2008). *Measurement of the Elastic Properties and Intrinsic Strength of Monolayer Graphene*. Science. 321: 385-388. doi: 10.1126/science.1157996

Li X, Wei W, Qin H, Hang Hu Y. (2015). *Co-effects of graphene oxide sheets and single wall carbon nanotubes on mechanical properties of cement*. Journal of Physics and Chemistry of Solids. 85: 39-43. doi:10.1016/J.JPCS.2015.04.018.

Lu Z, Li X, Hanif A, Chen B, Parthasarathy P, Yu J, Li Z. (2017). *Early-age interaction mechanism between the graphene oxide and cement hydrates*. Construction and Building Materials. 152: 232-239. doi:10.1016/j.conbuildmat.2017.06.176.

Lv S, Ting S, Liu J, Zhou Q. (2014). *Use of graphene oxide nanosheets to regulate the microstructure of hardened cement paste to increase its strength and toughness*. CrystEngComm. 16(36): 8508-8516. doi:10.1039/c4ce00684d.

Romani A. (2015). *Graphene Oxide as a cement reinforcement additive: Preliminary study*. (Thesis) Politecnico di Milano. pp:138.

Taylor HFW. (1998). *Cement Chemistry*. Volume 20. 2nd ed. Thomas Telford Publishing doi:10.1016/S0958-9465(98)00023-7.

Yang H, Cui H, Tang W, Li Z, Han N, Xing F. (2017). *A critical review on research progress of graphene/cement based composites*. Composites Part A: Applied Science and Manufacturing. 102: 273-296. doi:10.1016/J.COMPOSITESA.2017.07.019.

Zhao L, Guo X, Ge C, Li Q, Guo L, Shu X, Liu J. (2016). *Investigation of the effectiveness of PC@GO on the reinforcement for cement composites*. 113: 470-478. doi:10.1016/j.conbuildmat.2016.03.090.